Theory of orientation tuning in visual cortex

(neural networks/cross-correlations/symmetry breaking)

R. Ben-Yishai*, R. Lev Bar-Or*, and H. Sompolinsky†

*Racah Institute of Physics and Center for Neural Computation, Hebrew University, Jerusalem 91904, Israel; and †AT&T Bell Laboratories,
Murray Hill, NJ 07974

ABSTRACT The role of intrinsic cortical connections in processing sensory input and in generating behavioral output is poorly understood. We have examined this issue in the context of the tuning of neuronal responses in cortex to the orientation of a visual stimulus. We analytically study a simple network model that incorporates both orientation-selective input from the lateral geniculate nucleus and orientation-specific cortical interactions. Depending on the model parameters, the network exhibits orientation selectivity that originates from within the cortex, by a symmetry-breaking mechanism. In this case, the width of the orientation tuning can be sharp even if the lateral geniculate nucleus inputs are only weakly anisotropic. By using our model, several experimental consequences of this cortical mechanism of orientation tuning are derived. The tuning width is relatively independent of the contrast and angular anisotropy of the visual stimulus. The transient population response to changing of the stimulus orientation exhibits a slow "virtual rotation." Neuronal cross-correlations exhibit long time tails, the sign of which depends on the preferred orientations of the cells and the stimulus orientation.

Neurons in the primary visual cortex respond preferentially to edges with a particular orientation. The input to the cortex is provided by neurons in the lateral geniculate nucleus (LGN), which respond independently of the stimulus orientation. The mechanism for the generation of orientation selectivity in the cortex is not fully known (1–8). According to the classical model of Hubel and Wiesel (1), the preferred orientation (PO) of a cortical cell originates from the geometrical alignment of the circular receptive fields of the LGN neurons that are afferent to it. The experimental evidence of this model is ambiguous. The alignment of the receptive fields of the LGN inputs to a cortical cell apparently parallels the cell's PO (2). However, suppression of cortical inhibition tends to considerably degrade orientation tuning (3, 4), suggesting that cortical circuitry plays an important role in shaping the relatively sharp orientation tuning in the cortex. Furthermore, estimates based on intracellular measurements indicate that most of the orientation-selective excitatory input to cortical cells comes from cortical feedback (6). Several models implicating cortical inhibition have been proposed (for reviews, see refs. 7 and 8). Their analysis, however, is hindered by the need to resort to massive numerical simulations of the different models. Computational complexity also precluded a detailed study of the role of the cortical excitatory connections. An important constraint on modeling orientation selectivity, which has not yet been fully addressed, is the experimental finding that the tuning width is relatively insensitive to the contrast of the stimulus (9). Most experimental and theoretical studies of orientation selectivity focus on the response properties of single neurons. However, valuable insight into the cooperativity among cortical neurons can be gained from measurements of the correlations between the responses of different neurons (10). Theoretical predictions regarding the magnitude and form of correlation functions in neuronal networks have been lacking.

Here we study mechanisms for orientation selectivity by using a simple neural network model that captures the gross architecture of primary visual cortex. By assuming simplified neuronal stochastic dynamics, the network properties have been solved analytically, thereby providing a useful framework for the study of the roles of the input and the intrinsic connections in the formation of orientation tuning in the cortex. Furthermore, by using a recently developed theory of neuronal correlation functions in large stochastic networks, we have calculated the cross-correlations (CCs) between the neurons in the network. We show that different models of orientation selectivity may give rise to qualitatively different spatiotemporal patterns of neuronal correlations. These predictions can be tested experimentally.

Model

We consider a network model with an architecture of a cortical hypercolumn. It consists of N_E excitatory neurons and N_I inhibitory neurons that respond selectively to a small oriented visual stimulus in a common receptive field. The neurons are parameterized by an angle θ, ranging from $-\pi/2$ to $+\pi/2$, that denotes their POs. The interaction between a presynaptic excitatory neuron θ' and a postsynaptic excitatory or inhibitory neuron θ is equal to $N_E^{-1}E(\theta - \theta')$. Similarly, the interaction between a presynaptic inhibitory neuron and a postsynaptic neuron is $N_I^{-1}I(\theta - \theta')$. The functions $E(\theta - \theta')$ and $I(\theta - \theta')$ represent the fact that the strength of the interactions between two orientation columns depends on the difference between their POs. The synaptic input from the LGN to a neuron θ is denoted as $h^{ext}(\theta - \theta_0)$, where θ_0 is the orientation of the external stimulus. Neurons switch stochastically between a quiescent state [denoted as $S(\theta) = 0$], representing a state with background firing rate ($\approx$5 spikes per sec), and an active state [$S(\theta) = 1$], representing a state with saturated firing rate ($\approx$500 spikes per sec). The transition rates between these states are governed by a sigmoidal gain function, $g[h(\theta, t)]$, where $h(\theta, t)$ is the total synaptic input to the neuron θ at time t. By assuming that the number of neurons is large and that they cover uniformly all the angles, the activity profile in the network at time t can be represented by a continuous function $m(\theta, t)$, 0 $\leq m \leq 1$. This function denotes the mean activity level, relative to the saturation activity level, of the neurons with POs in the neighborhood of θ, at time t. Note that since the synaptic inputs to the excitatory and the inhibitory neurons in our model are the same, $m(\theta, t)$ describes the mean activity levels of both types of neurons.

In the limit of a large network, $m(\theta, t)$ obeys the following deterministic mean-field equations:

Abbreviations: LGN, lateral geniculate nucleus; PO, preferred orientation; CC, cross-correlation.

$$\tau_0 \frac{d}{dt} m(\theta, t) = -m(\theta, t) + g[h(\theta, t)], \qquad [1]$$

where τ_0 is a microscopic characteristic time (a few milliseconds), and the total synaptic input $h(\theta, t)$ is

$$h(\theta, t) = \int_{-\pi/2}^{+\pi/2} \frac{d\theta'}{\pi} J(\theta - \theta') m(\theta', t) + h^{\text{ext}}(\theta - \theta_0). \qquad [2]$$

Here $J(\theta - \theta')$ represents the net interaction between neurons θ and θ', i.e., $J(\theta - \theta') = E(\theta - \theta') + I(\theta - \theta')$. We choose $E(\theta) = E_0 + E_2\cos(2\theta)$ and $I(\theta) = -I_0 - I_2\cos(2\theta)$ with $E_0 \geq E_2 \geq 0, I_0 \geq I_2 \geq 0$. This choice implies that both the excitatory interactions and the inhibitory interactions are maximal for orientation columns with similar POs. This is in accord with the observation that the excitatory and inhibitory postsynaptic potentials to a cell have similar tuning (11, 12). The net interaction is

$$J(\theta) = -J_0 + J_2\cos(2\theta), \qquad [3]$$

with $J_0 = I_0 - E_0$ and $J_2 = E_2 - I_2$, both assumed to be positive. The constant J_0 represents a uniform all-to-all inhibition; J_2 measures the amplitude of the orientation-specific part of the interaction. Neurons with similar POs are more strongly coupled excitatorily than neurons with dissimilar ones. The external input is taken as

$$h^{\text{ext}}(\theta) = c[1 - \varepsilon + \varepsilon \cos(2\theta)], \qquad [4]$$

with $0 \leq \varepsilon \leq 1/2$. The parameter ε denotes the magnitude of the angular anisotropy of the input. The case $\varepsilon = 0$ denotes the limit where the input to the cortex is fully isotropic. The coefficient c measures the average amplitude of the input and will be referred to as the stimulus contrast. Finally, we use a semilinear gain function, i.e., $g(h) = 0$ for $h \leq T, g(h) = \beta(h - T)$ for $h \geq T$, and $g(h) = 1$ for $h \geq T + \beta^{-1}$. The parameter T is the threshold, which will be taken as 1, and β is the gain factor. This reflects the experimental finding that neuronal responses exhibit a sharp threshold contrast below which they vanish. Above threshold the mean firing rate of the neuron increases roughly linearly with the contrast. The slope of this rise is represented in our model by the constant β. Finally, the response saturates at high contrasts (13). The particular functional forms of the interactions, the LGN input and the gain function were chosen for the sake of simplicity. More general forms yield a behavior that is qualitatively similar to the present model.

Mechanisms for Orientation Selectivity

Mean-Field Solution. In the steady state, $m(\theta)$ is of the form $m(\theta) = M(\theta - \theta_0)$, where $M(\theta)$ peaks at $\theta = 0$. It represents the activity profile of the network relative to the orientation of the stimulus. Thus, $M(\theta)$ also represents the tuning curve of a neuron, centered at its PO. This function is given by the solution of the mean-field equation $M(\theta) = g[H(\theta)]$ with $H(\theta)$ being the local field, Eq. 2, centered at θ_0. Its value is $H(\theta) = (\varepsilon c + J_2 m_2)\cos(2\theta) + c(1 - \varepsilon) - J_0 m_0$, where m_0 and m_2 are the zeroth and the second Fourier coefficients of $M(\theta)$. The order parameter m_0 measures the neuronal activity averaged over the whole network, whereas m_2 measures the variation of this activity across the different columns. Self-consistent equations for m_0 and m_2 are derived by evaluating the Fourier transform of $M(\theta)$. The resultant form of $M(\theta)$ is $M(\theta) = \beta(\varepsilon c + J_2 m_2)[\cos(2\theta) - \cos(2\theta_C)]$ for $|\theta| < \theta_C$ and zero otherwise (see examples in Fig. 2). The cutoff angle θ_C, which is determined by the condition $H(\pm\theta_C) = 1$, is half of the full

width of the tuning curve and will be denoted as the tuning width. The above solution holds for suprathreshold contrast, $c > 1$. Otherwise, $M(\theta)$ is zero. In the following, we study the orientation tuning properties of the steady-state solution. In particular, we examine the dependence of the tuning width on the stimulus contrast, c, and anisotropy, ε, for different ranges of values of the connectivity parameters.

Hubel and Wiesel Scenario. The simplest scenario for orientation tuning is based on the Hubel–Wiesel mechanism. In the context of our model, this scenario corresponds to the case where the only synaptic input is coming from the LGN and this input is strongly anisotropic. Hence, the cortical local interaction $J(\theta)$ is zero and ε is substantially bigger than zero. The dependence of the tuning width θ_C on c in this case is shown in Fig. 1A for different values of ε. Near threshold (i.e., for $c \to 1$), θ_C vanishes, signaling the sharpening of the tuning width, relative to the input, by the thresholding operation of the cortical neurons. This, however, results in a strong dependence of the width on the contrast. As c increases, θ_C grows and beyond a certain value saturates at its maximum value $\pi/2$, which corresponds to the situation where all the neurons are activated by all stimuli.

Uniform Inhibition. A simple cortical mechanism for sharpening the orientation tuning is based on isotropic cortical inhibition. This scenario corresponds in our model to $J_0 > 0$ and $J_2 = 0$. In this case, the external input of each neuron has to overcome an effective enhanced threshold that increases with c because of the increase of the inhibitory feedback. Thus, even for $c \gg 1$, the inhibition may provide a sufficiently potent threshold to sharpen the tuning width. This is clearly seen in Fig. 1B (dashed line). Nevertheless, there is a strong dependence of the width on the contrast c. In addition, the width depends strongly on the anisotropy of the input, ε. In particular, when ε is small, $\theta_C = \pi/2$ for large c. This is shown in Fig. 1C (dashed line).

Marginal Phase. In the cases studied above, the anisotropy of the input to the cortex is the only source of orientation specificity. Can orientation specificity be generated by cortical interactions alone—even in the absence of significant anisotropy in the external input? To answer this question, we have studied the case of $\varepsilon = 0$ with J_0 and $J_2 > 0$. The assumed rotational symmetry of the cortex implies that when $\varepsilon = 0$, there is always a homogeneous solution, $M(\theta) = m_0$, which agrees with the naive expectation that the orientation tuning disappears when the external stimulus is isotropic. However, the equations yield also an inhomogeneous solution, provided that the angular modulation of the cortical interactions, J_2, is big enough, $J_2 > 2/\beta$. This solution represents a spontaneous generation of orientation tuning. It can be written as $m(\theta) = M(\theta - \phi)$, where the angle ϕ, which determines the location of the peak in $m(\theta)$, is arbitrary. This means that there is a continuum of stable states: they all have identical orientation tuned activity profiles, but they differ in the location of their peaks. The overall magnitude of $m(\theta)$ is determined by c but the shape of the activity profile is determined only by the cortical interactions. In particular, the width of $m(\theta)$ is independent of c but strongly depends on the magnitude of J_2. The bigger J_2, the smaller the width. We denote this solution a marginal phase because there are no barriers between the different attractors. This implies that the motion from one attractor to another is easier than motions in other directions of phase space. When the marginal solution exists, the naive homogeneous solution is unstable.

In reality, the location of the peak of the activity is not arbitrary but is determined by the orientation of the external input. Therefore, in a realistic implementation of the last scenario ε should be assumed to be small but nonzero. Since ε is small, the main effect of the anisotropy of the input is to select among the continuum of possible states that state in which the location of the peak in the activity matches the
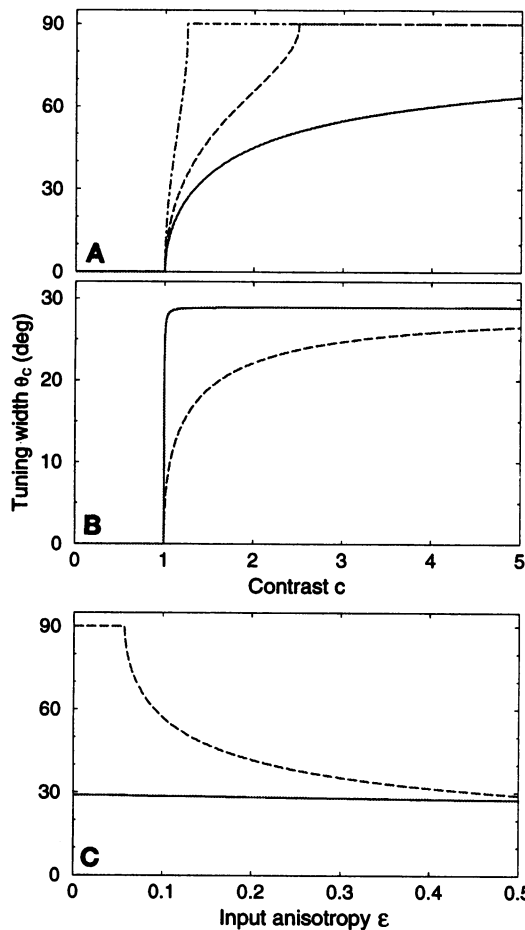
FIG. 1. Dependence of the orientation tuning with θ_C on the stimulus contrast and input anisotropy, for different mechanisms of tuning. The angle θ_C is the half-width of the tuning curve: neurons with POs of $>\theta_C$ away from the stimulus orientation are not activated. (*A*) The Hubel–Wiesel model, where the cortical interaction parameters J_0 and J_2 are zero. The tuning width is plotted against the contrast of the visual stimulus, c, for different values of the input anisotropy parameter, ε: ε = 0.1, 0.3, and 0.5 (dot-dashed, dashed, and solid lines, respectively). For $\varepsilon < 0.5$, there is a critical value of c above which θ_C = $\pi/2$, meaning that all neurons are activated by all stimuli. In the range where θ_C is small, it strongly depends on the level of contrast. Note that ε = 0.5 is the maximal value of anisotropy in our model. Here and in Figs. 2 and 3, β = 0.1. (*B*) Effect of cortical interactions on the tuning width. Dashed curve is for uniform cortical inhibition, with ε = 0.5, J_0 = 155, and J_2 = 0. The solid line is for parameters close to the marginal phase, where the tuning is dominated by the cortical interactions. In this case, θ_C saturates quickly to $\approx 30°$, while the level of maximal activity is still far from saturation (data not shown). Parameters are ε = 0.01, J_0 = 86, and J_2 = 112. They were chosen so that the value of θ_C agrees with the average value of the half-width for simple cells in the cat visual cortex (5). (*C*) The tuning width as a function of the input anisotropy in the limit $c \gg 1$. The solid line is for the marginal phase; the dashed curve is for the Hubel–Wiesel mechanism with uniform cortical inhibition. Parameters are as in *B*.

orientation of the stimulus, but it will not affect the shape of the tuning curve very much. This is indeed borne out by a solution of the mean-field equations with a small nonzero ε and large J_0 and J_2. There is a unique stable state, $m(\theta) = M(\theta - \theta_0)$, where $M(\theta)$ is approximately the same as for ε = 0. Whereas when ε = 0, θ_C was independent of c, and when ε is nonzero, θ_C vanishes as $c \to 1$. However, this decrease in θ_C occurs in a very narrow range of c near threshold, $c - 1 = O(\varepsilon)$, as shown in Fig. 1*B* (solid line). The value of θ_C for larger c is independent of c. It is also insensitive to changes in the value of ε, as shown in Fig. 1*C* (solid line).

Virtual Rotation

An interesting difference between the scenarios described above appears in the time-dependent response of the system to a change in the orientation of the external stimulus. Consider the case where the orientation of the external stimulus is changed at time 0 from $\theta_0 = \theta_1$ to $\theta_0 = \theta_2$. We assume that initially the stimulus was present long enough so that the system reached a steady-state $m(\theta)$ with a peak at $\theta = \theta_1$. How will the population activity respond to the change in orientation? In the case of isotropic cortical interactions ($J_2 = 0$), the initial activity profile that peaked at θ_1 decays in magnitude while another profile peaked at θ_2 grows, as shown in Fig. 2*A*. In the marginal phase, the response is drastically different. The population activity is $m(\theta, t) \approx M[\theta - \phi(t)]$, where $M(\theta)$ is the activity profile at steady state. We denote this solution as virtual rotation. The activity at time t is similar to that that
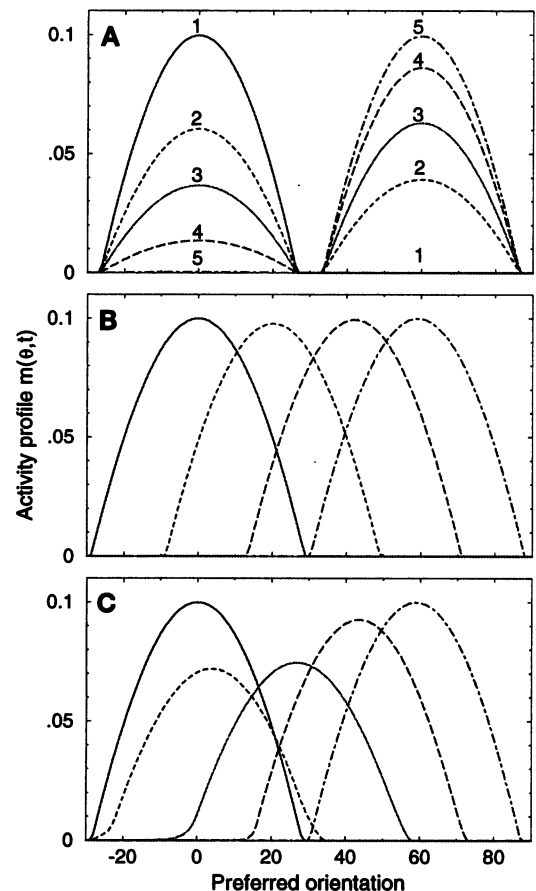
FIG. 2. Evolution of neuronal activity in response to a change in the stimulus orientation from an initial value $\theta_1 = 0°$ to $\theta_2 = 60°$. The change occurs at $t = 0$. (*A*) Hubel–Wiesel model with uniform inhibition. The activity profile centered at $0°$ decays while a new one, centered around $60°$, grows. Neurons in intermediate columns (e.g., with $\theta = 30°$) stay in the quiescent state during the whole process. The time constant of the decay and growth is τ_0. Times are 0, 0.5, 1, 2, and 6 τ_0 (lines 1–5, respectively). Parameters are as in Fig. 1*B* (dashed line) and $c = 5$. For this value of contrast, the maximal activity level relative to saturation is 0.1, which corresponds to a rate of ≈ 50 spikes per sec. (*B*) Virtual rotation in the marginal phase. The activity profile moves toward θ_2, activating successively the intermediate columns, and undergoing only very small changes during the process. $c = 1.678$; other parameters are as in Fig. 1*B* (solid line). Times are (left to right) 0, 90, 210, and 600 τ_0. (*C*) Virtual rotation accompanied by deformations in the activity profile. The magnitude of the deformations depends on the magnitude of ε. Here ε = 0.1, J_0 = 73, J_2 = 110, and c = 1.45. Times are (left to right) 0, 2, 10, 20, and 60 τ_0. By assuming $\tau_0 \approx 5$ msec, the predicted rotation velocity is 200 to 400°/sec.

would occur if there was an external stimulus with an orientation $\theta_0 = \phi(t)$. Substituting this form for $m(\theta, t)$ in the dynamic equations (Eqs. **1** and **2**), we find that the variable $\phi(t)$ obeys $\dot{\phi}(t) \approx -\omega_0 \sin[2\phi(t) - 2\theta_2]$, with $\phi(t = 0) = \theta_1$. The angular frequency ω_0 is given by

$$\omega_0 \tau_0 = \varepsilon c/(2J_2 m_2), \qquad [5]$$

where m_2 is the second Fourier coefficient of $M(\theta)$. Note that in the marginal phase m_2 remains finite even for small ε. Thus, ω_0, the angular velocity of the activity profile, is determined by the ratio of the modulation amplitudes of the external input and of the cortical synaptic input. This result is valid provided $\omega_0 \tau_0 = O(\varepsilon) \ll 1$. An example is shown in Fig. 2B, which corresponds to a marginal phase with $\varepsilon = 0.01$. The activity profile moves with an (initial) angular velocity $0.2°/\tau_0$, without significant change in its shape. Fig. 2C shows the case of $\varepsilon = 0.1$. Here, the angular velocity is faster by an order of magnitude, as predicted by Eq. **5**. In this case, the propagation of the activity is accompanied by significant transient changes in the amplitude of the activity profile.

CCs

The CC function $C(\theta, \theta'; \tau)$ measures the correlation between the temporal fluctuations in the rate of activity of a neuron θ at time t and that of another neuron, θ', at $t + \tau$. In our model, these fluctuations arise from the underlying stochasticity of the neuronal dynamics. The deterministic mean-field equations, Eq. **1**, neglect these small fluctuations. To study the CCs induced by these fluctuations, we have applied a recently developed theory of correlations in stochastic neural networks (14) and calculated analytically the CCs in our model for various parameter regimes. We consider here the CCs between excitatory neurons in the case of uniform inhibition and in the marginal phase. In the uniform inhibition case, the CCs are independent of θ, θ', and θ_0, as long as the two neurons are activated by the stimulus, and the CCs decay on a fast time scale, of the order of the microscopic time constant τ_0. This is shown in Fig. 3A. The results for the marginal phase are drastically different. Here, in addition to fast-decaying components, the CCs possess also a slow component that has the following unique dependence on θ, θ', and θ_0,

$$C(\theta, \theta', \tau) \propto \frac{1}{\varepsilon} \sin(2\theta - 2\theta_0)\sin(2\theta' - 2\theta_0)\exp(-\varepsilon|\tau|/\tau_0),$$

$$\tau \gg \tau_0. \qquad [6]$$

Thus, the longest decay time of the CCs is τ_0/ε, where ε is the amplitude of the angular modulation of the input, which is assumed to be small in this phase. The magnitude of the slow component is big, on the order of ε^{-1}. This slow component results from the fact that in the marginal phase, the noise induces random slow wandering of the system between neighboring attractors, thus generating small random virtual rotations.

The result (Eq. **6**) implies that not only the magnitude but also the sign of the CC between a pair of neurons may depend on the stimulus orientation. If the stimulus orientation is larger or smaller than both θ and θ', the CC is positive. On the other hand, if θ_0 is intermediate between the two POs, the CC is negative, despite the fact that the direct interaction between the two neurons is positive. These results are shown in Fig. 3 B–D, where we present the full CCs in the marginal phase. Comparing these results with Eq. **6**, it is seen that the properties of the CCs at short τ are affected by the contributions from the fast-decaying noncritical modes of fluctuations, which generate a narrow positive peak near the center. The long-time component is dominated by the critical mode.
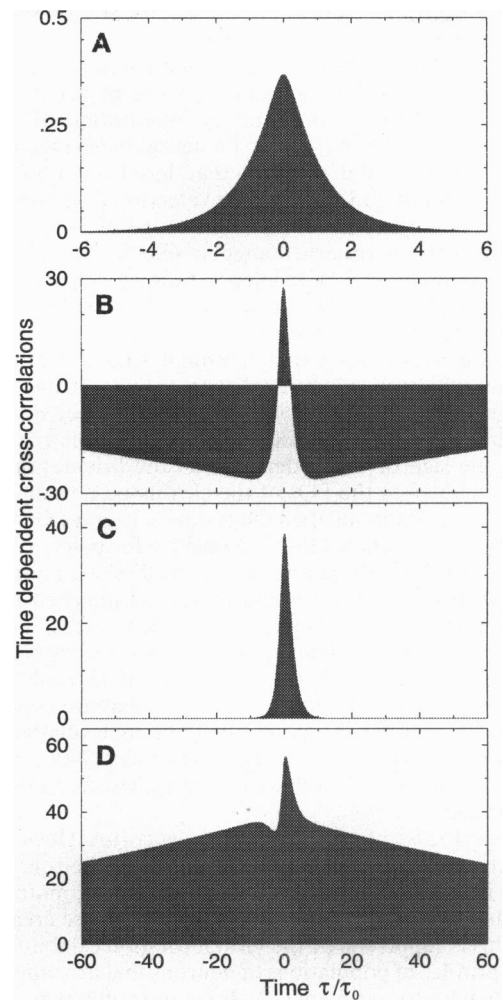
FIG. 3. Time-dependent CC between the fluctuations in the activity of two excitatory neurons, $\theta = -10°$ and $\theta' = 10°$, responding to a common oriented stimulus. (*A*) Uniform inhibition. The CC decay has a time constant on the order of τ_0. The CCs are independent of the stimulus orientation θ_0 (data not shown), as long as both neurons are activated by it. Parameters are as in Fig. 2A. The vertical scale displays the CCs multiplied by the number of excitatory neurons in the network, N_E. (*B–D*) CCs in the marginal phase for different stimulus orientations. Parameters are as in Fig. 2B. The CCs exhibit a slow-decaying component, with a time constant, τ_0/ε, and a magnitude that scales as ε^{-1}. (*B*) $\theta_0 = 0°$, i.e., between θ and θ', which results in a negative slow component, as predicted by Eq. **6**. (*C*) $\theta_0 = 10°$, for which the slow component vanishes. (*D*) $\theta_0 = 16°$, for which the slow component becomes positive.

Discussion

By using a simple neural network model, we have studied theoretically the consequences of different mechanisms for orientation selectivity in visual cortex. The network architecture is consistent with the known anatomy and physiology of visual cortex. In particular, the assumed angular modulation of the intracortical interactions, Eq. **3**, is supported by the spatial distributions of the dendritic and axonal arborizations in primary visual cortex (8). We find that if the amplitude of the cortical angular modulation, J_2, is sufficiently strong, the network can be in a state where the orientation tuning is dominated by the cortical circuitry. This state has several characteristic properties that can be verified experimentally. First, the tuning width is largely independent of stimulus properties such as its contrast and its degree of anisotropy. Indeed, invariance of the tuning width to contrast has been well documented (9). Measuring the effect of decreasing the

angular anisotropy of a stimulus on the orientation selectivity would be an additional important test.

The second characteristic, the virtual rotation, can be verified by measuring the transient response of primary visual cortex to an abrupt change in the orientation of a visual stimulus. Our model may suggest a neural mechanism for the psychophysical mental rotation that has been observed in object recognition (15). The initial velocities displayed in Fig. 2 *B* and *C*, assuming that τ_0 is in the range of 5–10 msec, are consistent with the observed angular velocity of mental rotation in psychophysical experiments, ranging between 60°/sec (15) and 400°/sec (16). Of course, other neuronal mechanisms for mental rotation are possible.

We have shown here that neuronal CCs are potentially important indicators of neuronal cooperativity. In our case, we predict that if cortical circuitry plays a dominant role in the orientation-selective response, CCs should exhibit a slow component, the sign of which depends on the orientation of the stimulus relative to the POs of the correlated neurons. If one averages over all stimuli, then the resultant average CCs should exhibit slow components that are positive for pairs of neurons with similar POs, and negative for largely dissimilar ones. Long time tails in CCs, which extend to several hundred milliseconds, are frequently observed in cortical areas, including primary visual cortex. Testing our theory requires systematic measurements of the slow components of CCs of pairs of neurons in different orientation columns that are coactivated by the same stimulus. Negative CCs, although relatively rare, have been observed in several cortical areas (17–20). Some of these correlations may be due to cooperative effects similar to those predicted here.

We have focused in this work on visual cortex. However, our approach can be applied also to the study of the role of local cortical interactions in other areas, primarily in motor areas, although the nature of the synaptic inputs to these areas is less clear. This is supported by the virtual rotation exhibited by the activity profiles of populations of neurons that are tuned to the direction of limb movement (17). Indeed, a network model that is similar to ours in some aspects was recently proposed for that system (21). It should be noted that the virtual rotation exhibited by our model is a direct outcome of the marginality of the network state and does not involve an active modulation of synapses, as in ref. 21. Also, the study of the neuronal correlations requires a more complex dynamics than the smooth deterministic model of ref. 21. As shown by our work, the correlations between a pair of neurons are not directly related to the value of the interactions between them. Instead, they are a consequence of the cooperative dynamical fluctuations in the network to which they belong.

Finally, we note that the marginal phase in the present theory is a result of the underlying angular symmetry of our model. It is thus similar to marginal phases that appear in physical systems at thermal equilibrium whenever a continuous symmetry is spontaneously broken. In particular, these systems exhibit "critical transverse correlations" that are similar to the slowly decaying CCs predicted here (22).

1. Hubel, D. H. & Wiesel, T. N. (1962) *J. Physiol. (London)* **160**, 106–154.
2. Chapman, B., Zahs, K. R. & Stryker, M. P. (1991) *J. Neurosci.* **11**, 1347–1358.
3. Tsumoto, T., Eckart, W. & Creutzfeldt, O. D. (1979) *Exp. Brain Res.* **34**, 351–363.
4. Sillito, A. M., Kemp, J. A., Milson, J. A. & Berardi, N. (1980) *Brain Res.* **194**, 517–520.
5. Orban, G. A. (1984) *Neuronal Operations in the Visual Cortex* (Springer, Berlin).
6. Ahmed, B. A., Anderson, J. C., Douglas, R. J., Martin, K. A. C. & Nelson, J. C. (1994) *J. Comp. Neurol.* **341**, 39–49.
7. Ferster, D. & Koch, D. (1987) *Trends Neurosci.* **10**, 487–492.
8. Martin, K. A. C. (1988) *Q. J. Exp. Physiol.* **73**, 637–702.
9. Skottun, B. C., Bradley, A., Sclar, G., Ohzawa, I. & Freeman, R. D. (1987) *J. Neurophysiol.* **57**, 773–786.
10. Fetz, E., Toyama, K. & Smith, W. (1991) in *Cerebral Cortex*, eds. Peters, A. & Jones, G. (Plenum, New York), Vol. 9.
11. Ferster, D. (1986) *J. Neurosci.* **6**, 1284–1301.
12. Douglas, R. J., Martin, K. A. C. & Whitteridge, D. (1991) *J. Physiol. (London)* **440**, 659–696.
13. Tolhurst, D. J., Movshon, J. A. & Thompson, I. D. (1981) *Exp. Brain Res.* **41**, 414–419.
14. Ginzburg, I. & Sompolinsky, H. (1994) *Phys. Rev. E* **50**, 3171–3191.
15. Shepard, R. N. & Metzler, J. (1971) *Science* **171**, 701–703.
16. Georgopoulos, A. P. & Massey, J. T. (1987) *Exp. Brain Res.* **65**, 361–370.
17. Georgopoulos, A. P., Taira, M. & Lukashin, A. (1993) *Science* **260**, 47–52.
18. Fetz, E. E. & Shupe, L. E. (1994) *Science* **263**, 1295–1296.
19. Hata, Y., Tsumoto, T., Sato, H., Hagihara, K. & Tamura, H. (1988) *Nature (London)* **335**, 815–817.
20. Vaadia, E., Haalman, I., Abeles, M., Bergman, H., Prut, Y., Slovin, H. & Aertsen, A. (1995) *Nature (London)* **373**, 515–518.
21. Lukashin, A. V. & Georgopoulos, A. P. (1993) *Biol. Cyber.* **69**, 517–524.
22. Forster, D. (1975) *Hydrodynamic Fluctuations, Broken Symmetry, and Correlation Functions* (Benjamin, Reading, MA).